

Rotational line strengths and self-pressure-broadening coefficients for the 1.27- μm , $a^1\Delta_g-X^3\Sigma_g^-, v=0-0$ band of O_2

Walter J. Lafferty, Alexander M. Solodov, Catherine L. Lugez, and Gerald T. Fraser

We measured at 296 K the rotational line strengths and pressure-broadening coefficients for the 1.27- μm , $a^1\Delta_g-X^3\Sigma_g^-, v=0-0$ band of O_2 with a Fourier transform infrared spectrometer using an optical path length of 84 m, a spectral resolution of 0.01 cm^{-1} , and sample pressures between 13 and 104 kPa. The integrated band strength is $7.79(17) \times 10^{-6}\text{ m}^{-2}\text{ Pa}^{-1}$ [$7.89(17) \times 10^{-5}\text{ cm}^{-2}\text{ atm}^{-1}$], and the Einstein A coefficient for spontaneous emission is $2.237(51) \times 10^{-4}\text{ s}^{-1}$, which corresponds to an upper-state $1/e$ lifetime of 1.24(3) h. The pressure-broadening coefficients decrease with increasing N and range from 19 to 38 MHz/kPa (FWHM). The mean value for the transitions studied is 30.3(21) MHz/kPa [$0.1024(71)\text{ cm}^{-1}/\text{atm}$] (FWHM). The Einstein A coefficient determined here is in good agreement with the widely accepted value of $2.58 \times 10^{-4}\text{ s}^{-1}$ initially obtained by Badger *et al.* [J. Chem. Phys. **43**, 4345 (1965)] more than 30 years ago. The standard uncertainties given above are one standard deviation.

OCIS codes: 010.1320, 010.4950, 020.3690, 300.6300, 300.1030, 010.0010.

1. Introduction

The 1.27- μm (7882-cm^{-1}) $a^1\Delta_g-X^3\Sigma_g^-, v=0-0$ band of O_2 plays an important role in atmospheric chemistry and physics. On the Earth the band is observed from the ground in absorption against the solar background¹ and in emission from the twilight airglow.² The electronically excited $a^1\Delta_g$ O_2 responsible for the airglow is predominantly produced by solar photolysis of O_3 by means of the Hartley bands. This fact has led to efforts to determine indirectly O_3 concentrations in the mesosphere and thermosphere by satellite monitoring of the 1.27- μm emission. The Solar Mesosphere Explorer satellite³ and the soon-to-be-launched Thermosphere Ionosphere Mesosphere Energetics and Dynamics satellite⁴ follow this approach. Extraterrestrial studies have also used the 1.27- μm band. Ground-based measurements of O_3 variations in the Martian atmosphere have been made by monitoring the 1.27- μm emission from the planet.⁵

In addition to being a signature of O_3 production, the 1.27- μm band of O_2 is also important for heating

the upper atmosphere. Mlynczak and Marshall⁶ studied atmospheric heating by solar absorption through the $b^1\Sigma_g^+-X^3\Sigma_g^-$ band system and the $a^1\Delta_g-X^3\Sigma_g^-$ band and found that together these bands contribute approximately 10% to the diabatic heating of the middle mesosphere. The $a^1\Delta_g-X^3\Sigma_g^-$ band itself is responsible for $\sim 10\%$ of the O_2 -contributed heating of the tropopause.⁶

To use the 1.27- μm band for atmospheric modeling and sensing, one must have accurate spectroscopic parameters for the band. The need for accurate 1.27- μm parameters was addressed by Mlynczak and Olander⁷ in a detailed assessment of the O_3 atmospheric concentration retrieval discussed above. Their analysis shows that, for altitudes between approximately 30 and 75 km, a 15% error in the Einstein A coefficient for spontaneous emission by $a^1\Delta_g$ O_2 gives a similar error in the retrieved O_3 concentration. The possibility of a large error in the accepted value for the Einstein A coefficient for $a^1\Delta_g$ O_2 was recently suggested by Mlynczak and Nesbitt.⁸

Despite the obvious importance of the 1.27- μm band in atmospheric studies, only a few laboratory measurements of the absorption spectrum of the 1.27- μm band of O_2 have been reported previously, mainly because of the small intensity of this magnetic-dipole-allowed band. Evidence of the weakness of this band is seen in the very long radiative lifetime of the $a^1\Delta_g$ state of $\tau_{1/2} \sim 45$ min, as

The authors are with the Optical Technology Division, National Institute of Standards and Technology, Gaithersburg, Maryland 20899.

Received 18 August 1997; revised manuscript received 3 November 1997.

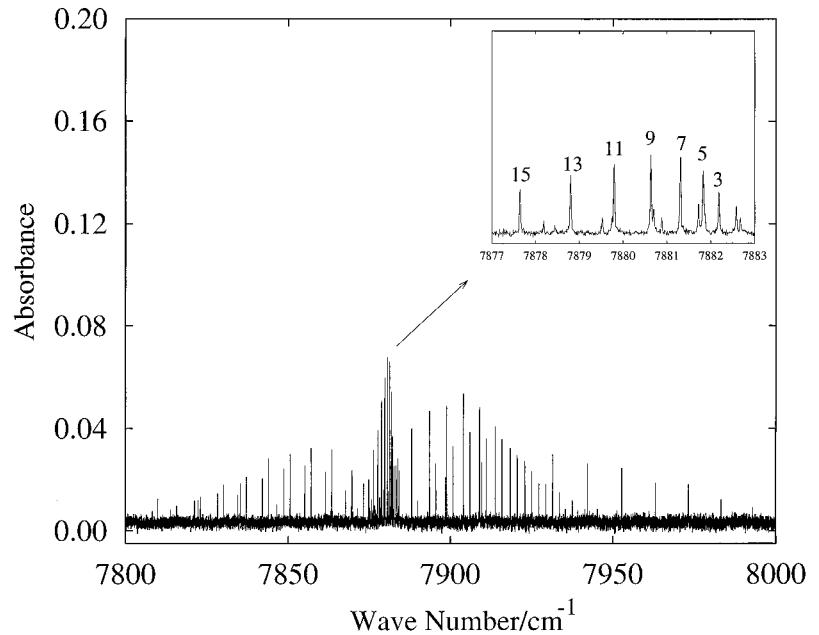


Fig. 1. Fourier transform infrared spectrum of the 1.27- μm (7882-cm^{-1}) $a^1\Delta_g-X^3\Sigma_g^-, v = 0-0$ band of O_2 . A logarithm base- e absorbance scale is used. We recorded the spectrum at 0.01-cm^{-1} resolution using a path length of 84.05 m, a sample pressure of 13.34 kPa, and a sample temperature of 296 K. The region near the qQ branch is expanded in the insert.

inferred by Badger *et al.*⁹ from measurements of the absolute integrated absorption intensity of the 1.27- μm band with a 1-m grating spectrometer and an optical path length of 32 m. More recently, Hsu *et al.*¹⁰ reported a Fourier transform infrared spectrum of the 1.27- μm band at pressures as high as 101 kPa and an optical path length of 18.75 m. These measurements refined previous results that they obtained¹¹ and were used by Mlynczak and Nesbitt⁸ to calculate an Einstein A coefficient for spontaneous emission of $1.47 \times 10^{-4} \text{ s}^{-1}$. This A value is smaller by a factor of 1.75 times than the widely accepted value of Badger *et al.*⁹ determined 30 years earlier. More recently, Pendleton *et al.*¹² challenged the Hsu *et al.*¹⁰ results by presenting a reanalysis of the time decay of the twilight atmospheric emission associated with the 1.27- μm band. Their results support a radiative lifetime in agreement with Badger *et al.*⁹ Also, Gamache *et al.*¹³ obtained results in agreement with Badger *et al.*⁹ from analysis of the solar spectrum.

Here we report laboratory measurements of the rotational line strengths and self-pressure-broadening coefficients for the 1.27- μm $a^1\Delta_g-X^3\Sigma_g^-, v = 0-0$ band of O_2 using a long-path-length (84 m), high-pressure (13–104 kPa) White cell and a high-resolution (0.01-cm^{-1}) Fourier transform infrared spectrometer. Accurate line frequencies and rotational constants are available for this band from several studies, including laboratory Fourier transform infrared emission studies at 1.27 μm ,¹⁴ pure rotational spectra of the ground¹⁵ and electronically excited states,¹⁶ and high-resolution stimulated Raman studies of the electronic ground state.¹⁷ Our analysis determines an Einstein A coefficient for 1.27- μm emission by $a^1\Delta_g$ O_2 of $2.226(50) \times 10^{-4} \text{ s}^{-1}$ (uncertainties are one standard deviation), which agrees to

within $\sim 15\%$ with the earlier measurement of Badger *et al.*⁹ The present measurement is larger by a factor of 1.5 than the $1.47 \times 10^{-4} \text{ s}^{-1}$ value of Hsu *et al.*,¹⁰ as corrected by Mlynczak and Nesbitt.⁸ Our integrated band intensity differs by $\sim 15\%$ from the value used in the HITRAN96¹⁸ atmospheric spectral database, which is based on the Einstein A coefficient of Gamache *et al.*¹³ of $2.59 \times 10^{-4} \text{ s}^{-1}$ determined from an analysis of the solar spectrum of Wallace and Livingston.¹⁹

2. Experimental

We recorded spectra using a Bomem DA3.002 Fourier transform spectrometer coupled to a long-path White-type absorption cell described by Tobin *et al.*²⁰ We measured all spectra at 0.01-cm^{-1} resolution using a CaF_2 beam splitter, an InSb detector, and a sample path length of 84.05 m. Five spectra were recorded at O_2 sample pressures from 13 to 104 kPa and a sample temperature of 296 K. The sample pressures are known to 0.1%, the path length is known to better than 0.01%, and the temperature is known to better than 0.3%. Spectra recorded at the lowest and highest pressures are shown in Figs. 1 and 2.

We obtained line intensities and widths by fitting the observed transitions to a Voigt line-shape profile with the Gaussian component fixed at the calculated Doppler width [$515 (\nu/\nu_0)$ MHz or $0.01718 (\nu/\nu_0) \text{ cm}^{-1}$ FWHM for $\nu_0 = 7883.8 \text{ cm}^{-1}$]. Individual lines were independently fitted except near the band center, where the high line density required several lines to be fitted at once. Because of the weakness of the lines and the uncertainty in the baseline position, we fitted each peak three times using different estimates of the input parameters (i.e., linewidth, line center, intensity, and baseline) to the fit. The reported

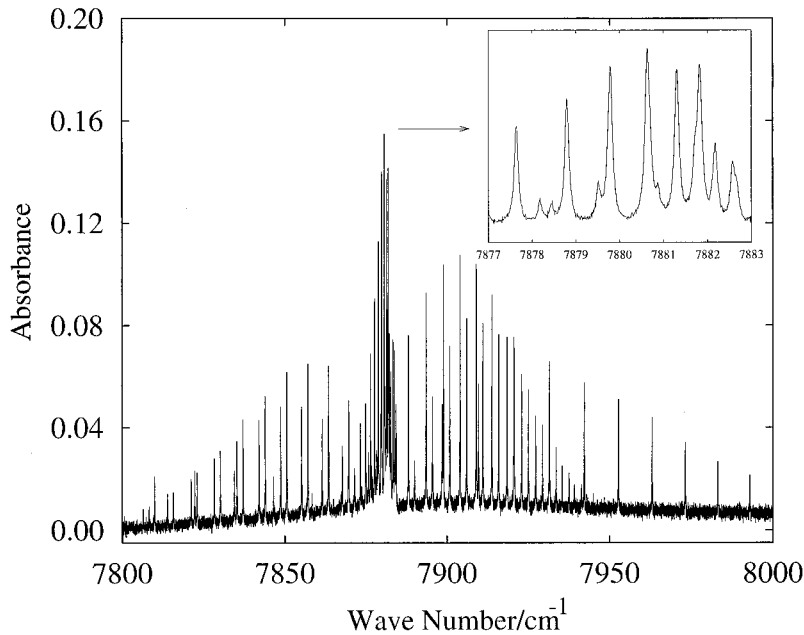


Fig. 2. Fourier transform infrared spectrum of the 1.27- μm (7882-cm^{-1}) $\alpha^1\Delta_g-X^3\Sigma_g^-, v = 0-0$ band of O_2 . The conditions are the same as those in Fig. 1 except for the sample pressure, which is 104.3 kPa. The small offset in the baseline is attributed to the collision-induced absorption continuum.

numbers are based on the average of the three results. The slope from a linear fit of transition intensity versus pressure determines the line strength of a transition, and the slope from the fit of Lorentzian linewidth versus pressure yields the pressure-broadening coefficient. Owing to the lack of correction for the instrumental resolution of 0.01 cm^{-1} , the pressure-broadening linewidth versus pressure plots do not intersect at the origin. Model calculations indicate that the neglect of the instrumental width leads to an error of $\sim 2\%$ in the reported broadening coefficients. This error is less than the typical uncertainty on a reported broadening coefficient.

3. Results

The measured integrated absorption coefficients and pressure-broadening coefficients for the individual rotational lines of the $\alpha^1\Delta_g-X^3\Sigma_g^-, v = 0-0$ band of O_2 are listed in Table 1. Badly blended lines, which occur mainly near the band origin, were excluded from the table. The uncertainties are the standard deviations (type-A standard uncertainties) from a linear least-squares fit of the intensities or linewidths as a function of pressure.

The integrated absorption coefficient for an electronic transition between lower state j and upper state i is given by

$$\int \alpha_\nu d\nu = \frac{2\pi^2}{3\epsilon_0 hc} \frac{1}{2J_j + 1} f_j n \nu_{ij} S_{ij}, \quad (1)$$

where J_j is the total angular momentum of the lower state, n is the number of molecules per unit volume, f_j is the fraction of molecules in state j , and S_{ij} is the line strength. The fraction f_j is obtained from

$$f_j = \frac{C_{\text{isotopic}}}{Q_v Q_{\text{rot}}} (2J_j + 1) \exp(-E_j/kT), \quad (2)$$

where Q_{rot} is the rotational partition function summed over the three spin components of the $S = 1$ ground state, Q_v is the vibrational partition function, C_{isotopic} is the isotopic abundance of the isotopomer studied, and E_j is the energy of the lower state. The thermal population of excited electronic states is effectively zero and is ignored. At 296 K, $Q_{\text{rot}} = 215.367$ when the zero of rotational energy is chosen so that the $F_1(N = 0, J = 1)$ level has an energy of -0.450179 cm^{-1} and $Q_v = 1.0005$ when the zero of vibrational energy is chosen as the $v = 0$ state. For $^{16}\text{O}_2$, $C_{\text{isotopic}} = 0.995186$.

The line-strength factors S_{ij} consist of sums of transition-dipole-moment matrix elements over the three spatial directions and over the degenerate M_J components of the upper and lower states. We express the S_{ij} as

$$S_{ij} = \mu_\perp^2 q_{\nu\nu'} L_{ij}, \quad (3)$$

where μ_\perp is a transition-moment matrix element, $q_{\nu\nu'}$ is a Franck-Condon factor, and L_{ij} is the rotational line intensity factor. Here we follow the recommendations of Whiting *et al.*²¹ and choose as our transition moment operators $(\mu_x \pm i\mu_y)/2^{1/2}$, where μ_x and μ_y are the projections of the transition moment onto the body-fixed x and y axes. With this convention, $\mu_\perp = \langle \Omega = \pm 2 | (\mu_x \pm i\mu_y)/2^{1/2} | \Omega = \pm 1 \rangle$, and the L_{ij} for all transitions from a given set of J levels sum to $6(2J + 1)$ (ignoring statistical weights) when the rules of Whiting *et al.* are used.²² Note that our L_{ij} are larger by a factor of 2 than those of Balasubramanian and Bellary,^{23,24} who define $\mu_\perp = \langle \Omega = \pm 2 | \mu_x \pm i\mu_y | \Omega = \pm 1 \rangle$. In the above expressions for the line strengths we ignore the effects of rotation-vibration and rotation-electronic couplings²³ on the transition moments.

Lower-state constants needed for the evaluation of

Table 1. Rotational Line Strengths, Integrated Band Intensities, and Self-Pressure-Broadening Widths for the $a^1\Delta_g-X^3\Sigma_g^-$ Band of O_2 at 296 K^{a,b}

| Transition | S_{ij} | | S_v | Γ (FWHM) | |
|--------------------|--|--|---------|--|-----------------------|
| | $10^{-7} \text{ m}^{-2} \text{ Pa}^{-1}$ | $10^{-6} \text{ cm}^{-2} \text{ atm}^{-1}$ | | $10^{-6} \text{ m}^{-2} \text{ Pa}^{-1}$ | MHz kPa ⁻¹ |
| ^s R(3) | 0.966(9) | 0.979(9) [1.362] | 7.41(7) | 32(2) | 0.107(5) |
| ^s R(9) | 1.024(6) | 1.037(7) [1.247] | 7.79(5) | 29(2) | 0.099(5) |
| ^s R(11) | 0.87(1) | 0.89(1) [1.049] | 7.79(9) | 30.9(7) | 0.104(2) |
| ^s R(13) | 0.718(9) | 0.727(9) [0.824] | 8.0(1) | 30.3(9) | 0.103(3) |
| ^s R(15) | 0.518(8) | 0.525(8) [0.606] | 7.8(1) | 29(2) | 0.099(8) |
| ^s R(17) | 0.37(1) | 0.37(1) [0.418] | 8.0(3) | 23(5) | 0.08(2) |
| ^s R(19) | 0.219(7) | 0.222(8) [0.271] | 7.3(2) | 25(3) | 0.09(1) |
| ^r R(1) | 1.61(2) | 1.63(2) [1.868] | 7.80(9) | 37.6(7) | 0.127(3) |
| ^r R(3) | 1.86(1) | 1.88(1) [2.177] | 7.73(5) | 32(1) | 0.108(3) |
| ^r R(7) | 2.05(2) | 2.08(2) [2.395] | 7.74(6) | 31(1) | 0.105(4) |
| ^r R(9) | 1.90(1) | 1.93(1) [2.213] | 7.75(6) | 31(1) | 0.103(3) |
| ^r R(11) | 1.622(3) | 1.644(3) [1.894] | 7.70(1) | 29.7(7) | 0.100(2) |
| ^r R(13) | 1.31(1) | 1.33(1) [1.508] | 7.79(6) | 29(2) | 0.099(5) |
| ^r R(15) | 1.00(1) | 1.01(1) [1.121] | 7.97(8) | 30(1) | 0.102(5) |
| ^r R(17) | 0.669(8) | 0.678(9) [0.780] | 7.7(1) | 26.6(9) | 0.090(3) |
| ^r Q(1) | 0.43(1) | 0.43(1) [0.629] | 8.0(2) | 39(3) | 0.131(9) |
| ^r Q(5) | 1.351(9) | 1.369(9) [1.720] | 7.87(5) | 32(1) | 0.109(4) |
| ^r Q(7) | 1.50(1) | 1.52(1) [1.880] | 7.77(7) | 32(1) | 0.107(4) |
| ^r Q(9) | 1.469(9) | 1.488(9) [1.828] | 7.71(5) | 30.0(5) | 0.101(2) |
| ^r Q(11) | 1.29(1) | 1.31(1) [1.618] | 7.58(7) | 32(1) | 0.108(4) |
| ^r Q(15) | 0.834(5) | 0.845(5) [0.999] | 7.79(4) | 25(1) | 0.085(3) |
| ^r Q(17) | 0.577(5) | 0.585(5) [0.705] | 7.59(6) | 26.8(9) | 0.091(3) |
| ^r Q(19) | 0.400(1) | 0.405(1) [0.465] | 7.93(2) | 29(3) | 0.097(9) |
| ^q R(17) | 0.303(8) | 0.307(8) [0.368] | 7.2(2) | 28(1) | 0.096(4) |
| ^q R(19) | 0.178(6) | 0.180(6) [0.243] | 6.4(2) | 19(1) | 0.066(5) |
| ^q Q(13) | 2.42(8) | 2.45(8) [2.373] | 9.3(3) | 29(1) | 0.099(3) |
| ^q Q(15) | 1.55(2) | 1.57(2) [1.824] | 7.8(1) | 29.4(2) | 0.0994(8) |
| ^q Q(17) | 1.05(1) | 1.07(1) [1.302] | 7.38(8) | 28(1) | 0.095(4) |
| ^q Q(21) | 0.549(8) | 0.556(8) [0.541] | 9.3(1) | 27(2) | 0.090(6) |
| ^q P(17) | 0.2(1) | 0.2(1) [0.293] | 7(5) | 24(5) | 0.08(2) |
| ^p Q(7) | 1.17(1) | 1.19(1) [0.241] | 7.75(7) | 32(1) | 0.107(4) |
| ^p Q(9) | 1.22(1) | 1.24(1) [1.334] | 7.75(9) | 31(1) | 0.105(4) |
| ^p Q(11) | 1.15(2) | 1.17(2) [1.258] | 7.9(1) | 31.5(1) | 0.1064(4) |
| ^p Q(13) | 0.973(8) | 0.986(8) [1.072] | 7.93(7) | 30(2) | 0.103(6) |
| ^p Q(15) | 0.754(8) | 0.764(8) [0.839] | 7.93(9) | 29.0(9) | 0.098(3) |
| ^p Q(17) | 0.543(8) | 0.551(8) [0.607] | 8.0(1) | 30(2) | 0.100(6) |
| ^p Q(19) | 0.395(5) | 0.400(6) [0.409] | 8.6(1) | 26.7(2) | 0.0901(8) |
| ^p Q(21) | 0.23(1) | 0.23(1) [0.257] | 8.0(4) | 33(2) | 0.112(8) |
| ^p Q(23) | 0.139(6) | 0.141(6) [0.152] | 8.3(3) | | |
| ^p P(5) | 0.514(5) | 0.521(6) [0.618] | 7.60(8) | 31.3(9) | 0.106(3) |
| ^p P(7) | 0.76(1) | 0.77(1) [0.922] | 7.5(1) | 28(4) | 0.09(1) |
| ^p P(9) | 0.900(8) | 0.912(8) [1.058] | 7.82(7) | 32.3(7) | 0.109(3) |
| ^p P(11) | 0.881(5) | 0.893(6) [1.039] | 7.82(5) | 31(2) | 0.106(5) |
| ^p P(13) | 0.762(5) | 0.773(6) [0.911] | 7.73(5) | 29.5(7) | 0.099(2) |
| ^p P(15) | 0.60(1) | 0.61(1) [0.727] | 7.6(1) | 27(3) | 0.092(9) |
| ^p P(19) | 0.301(8) | 0.305(8) [0.365] | 7.7(2) | 29(2) | 0.098(5) |
| ^p P(21) | 0.209(9) | 0.212(9) [0.232] | 8.4(3) | 28(1) | 0.093(4) |
| ^o P(5) | 0.16(1) | 0.16(1) [0.174] | 7.2(6) | | |
| ^o P(7) | 0.32(8) | 0.33(1) [0.336] | 7.9(3) | 31(3) | 0.11(1) |
| ^o P(9) | 0.38(1) | 0.38(1) [0.426] | 7.6(2) | 31(2) | 0.104(8) |
| ^o P(11) | 0.373(5) | 0.378(6) [0.442] | 7.3(1) | 28.4(9) | 0.096(3) |
| ^o P(13) | 0.354(8) | 0.359(8) [0.402] | 7.8(2) | 28(4) | 0.09(1) |

^aOne standard uncertainties are given.

^bNumbers in brackets are HITRAN96 values¹⁷ in units of $10^{-6} \text{ cm}^{-2} \text{ atm}^{-1}$.

L_{ij} , Q_r , ν_{ij} , ν_0 , and E_i are obtained from the Hamiltonian of Rouillé *et al.*,¹⁷ whereas upper-state rotational constants are determined by a fit of the microwave measurements of Hillig *et al.*¹⁶ to B and D_J . The band origin is taken from the results of Amiot and Verges.¹⁴

Using Eqs. (1)–(3), one can determine the theoretical fractional contribution of each rovibronic transition to the total integrated band strength for $\nu = 0$, $^{16}O_2$ by dividing the calculated rovibronic line intensities by the sum of all the calculated line intensities. Dividing the experimental line strength by its frac-

tional contribution gives a value for the integrated band strength S_v consistent with the observed intensity of the line. The integrated band strengths S_v determined from each of the individual lines are listed in Table 1. Theoretically, we expect the fractional contributions of the oP , pQ , qR , qP , rQ , sR , pP , qQ , and rR subbands to the total integrated band intensity to be 0.032, 0.103, 0.083, 0.044, 0.135, 0.104, 0.075, 0.230, and 0.195, respectively. Consistent with these fractional intensities, the dominant transitions in Figs. 1 and 2 arise from the qQ branch.

An alternative procedure for determining the integrated band strength by summing of the experimentally determined absorption coefficients of the individual lines, as performed by Hsu *et al.*,¹⁰ can lead to significant errors, depending on the signal-to-noise ratio of the measurements. For example, we calculate that Hsu *et al.*¹⁰ included only approximately 95% of the theoretical band intensity in their sum, which was limited to lower-state N values of 23 or less. Another alternative approach that involves numerical integration of the observed spectrum can lead to errors because of the poor signal-to-noise ratio and the difficulty of specifying the baseline precisely, owing to the weak collision-induced absorption background, particularly at the higher pressures.

A weighted average of the S_v listed in Table 1 (with the weight factor proportional to the square of the reciprocal uncertainty on the S_v value) gives $7.75(17) \times 10^{-6} \text{ m}^{-2} \text{ Pa}^{-1}$ [$7.85(17) \times 10^{-5} \text{ cm}^{-2} \text{ atm}^{-1}$ or $3.166(69) \times 10^{-24} \text{ cm molecule}^{-1}$] for the integrated band strength of the $v = 0-0$ component of ${}^{16}\text{O}_2$ at 296 K, where the pressure units refer to a sample of O_2 of natural isotopic composition. Including contributions from the other isotopic forms by assuming that the matrix elements of the transition-moment operator are isotope independent gives an integrated band strength of $7.79(17) \times 10^{-6} \text{ m}^{-2} \text{ Pa}^{-1}$ [$7.89(17) \times 10^{-5} \text{ cm}^{-2} \text{ atm}^{-1}$ or $3.182(69) \times 10^{-24} \text{ cm molecule}^{-1}$]. This S_v value corresponds to an Einstein B coefficient of $61.0(14) \text{ m}^2 \text{ J}^{-1} \text{ s}^{-1}$ and an Einstein A coefficient of $2.237(51) \times 10^{-4} \text{ s}^{-1}$ for the $v = 0-0$ component of the band. In the calculations of the Einstein A coefficient we used an upper-to-lower-state degeneracy ratio of 1.5, as discussed by Herzberg²⁵ and Mlynczak and Nesbitt.⁸ The corresponding upper-state $1/e$ lifetime is $1.24(3) \text{ h}$.

From the magnitude of the Einstein A coefficient we can also determine the value of the transition-moment matrix element. From the definition of μ_{\perp} given above we find that

$$A = \frac{1}{4\pi\epsilon_0} \left(\frac{64\pi^4\nu_0^3}{h} \right) \mu_{\perp}^2 q_{vv'}, \quad (4)$$

where $\nu_0 = 7883.76 \text{ cm}^{-1}$ is the $v = 0-0$ band origin. For a magnetic-dipole-allowed transition we obtain a value of $q_{vv'}^{1/2} \mu_{\perp} = 2.21(3) \times 10^{-26} \text{ J T}^{-1}$ [$2.38(3) \times 10^{-3} \mu_B$]. If we assume hypothetically that the transition is electric-dipole allowed, we obtain a transition moment of $7.3(7) \times 10^{-35} \text{ C m}$ [$2.20(2) \times 10^{-5} \text{ D}$].

The weighted average of the tabulated pressure-

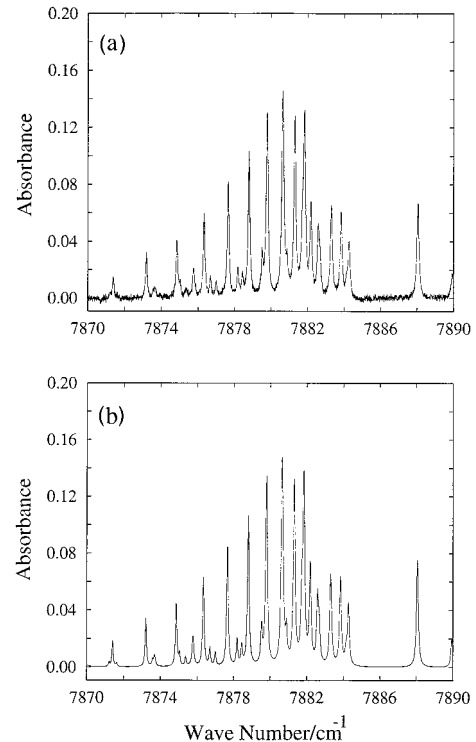


Fig. 3. (a) Observed and (b) calculated spectra in the Q -branch region of the $\alpha^1\Delta_g-X^3\Sigma_g^-, v = 0-0$ band of O_2 . A logarithm base- e absorbance scale is used. The experimental spectrum is the same as that in Fig. 2. The simulation uses a Voigt line-shape profile with an N -dependent Lorentzian linewidth, as described in the text; a Gaussian Doppler FWHM of $0.01718 (\nu/\nu_0) \text{ cm}^{-1}$ for $\nu_0 = 7883.8 \text{ cm}^{-1}$, and an integrated band strength of $7.75 \times 10^{-6} \text{ m}^{-2} \text{ Pa}^{-1}$ for a path length of 84.05 cm and a pressure of 104.3 kPa .

broadening coefficients Γ in Table 1 gives a self-broadening coefficient of $30.3(21) \text{ MHz/kPa}$ [$0.1024(71) \text{ cm}^{-1}/\text{atm}$] (FWHM) at 296 K. This pressure-broadening coefficient is in good agreement with the value of $30(3) \text{ MHz/kPa}$ (FWHM) determined by Hsu *et al.*¹⁰ at 300 K. Closer examination of the data in Table 1 reveals that the pressure-broadening coefficients vary with rotational angular momentum approximately as

$$\Gamma = \Gamma_0 + \Delta_{\Gamma}[N''(N'' + 1) + J'(J' + 1) - 4]/2, \quad (5)$$

where $\Gamma_0 = 33.6(3) \text{ MHz/kPa}$ [$0.1137(9) \text{ cm}^{-1}/\text{atm}$] and $\Delta_{\Gamma} = -0.019(1) \text{ MHz/kPa}$ [$-6.4(5) \times 10^{-5} \text{ cm}^{-1}/\text{atm}$] at 296 K for $N'' \leq 23$. The measured average pressure-broadening parameter and line strength were used to simulate the Q -branch region of the spectrum, as shown in Fig. 3. Examination of Fig. 3 indicates that the average broadening and line-strength values lead to peak intensities for most of the lines between 7880 and 7890 cm^{-1} , which are slightly too high. The peak intensities between 7870 and 7880 cm^{-1} , however, are in good agreement with the simulation.

4. Discussion

The present Einstein A coefficient of $2.237(51) \times 10^{-4} \text{ s}^{-1}$ is in reasonable agreement with the widely accepted value of $2.58 \times 10^{-4} \text{ s}^{-1}$ determined by Badger *et al.*⁹ from laboratory measurements with a 1-m grating spectrometer that had a sample optical path length of 32 m, and it is also in reasonable agreement with the $2.59 \times 10^{-4} \text{ s}^{-1}$ value determined by Gamache *et al.*¹³ from an analysis of the solar spectrum of Wallace and Livingston.¹⁹ The radiative lifetime obtained from the present measurements is also in good agreement with the approximately 1-h lifetime inferred from analysis of the time dependence of the 1.27- μm atmospheric emission by Pendleton *et al.*,¹² Gattinger and Vallance Jones,²⁶ and Evans *et al.*²⁷ Our A value is in poor agreement with the $1.47 \times 10^{-4} \text{ s}^{-1}$ value of Hsu *et al.*,¹⁰ as corrected by Mlynczak and Nesbitt.⁸ The Hsu *et al.*¹⁰ value is clearly too low to be consistent with the results from the numerous atmospheric studies, as noted by Pendleton *et al.*¹²

The origin of the error in the Hsu *et al.*¹⁰ study is not clear; however, their most recent measurement gives an integrated band strength that is larger by a factor of ~ 2 than a measurement that two of the authors reported earlier¹¹ at a reduced signal-to-noise ratio using the same spectrometer. Note further that our sensitivity is higher, largely owing to the longer path length of 84 m compared with the 18.75-m path length used by Hsu *et al.*¹⁰ An indication of our higher sensitivity is the ability to observe the collision-induced absorption background, as shown in Fig. 2, which was not seen by Hsu *et al.*¹⁰ Indeed, future efforts will be directed at further characterizing the contribution of the collision-induced absorption to the radiative lifetime of the upper state.

The authors acknowledge Aaron Goldman for sharing results from his research with us. This study has been partially supported by the NASA Upper Atmosphere Research Program.

References

1. L. Herzberg and G. Herzberg, "Fine structure of the infrared atmospheric oxygen bands," *Astrophys. J.* **105**, 353–359 (1947).
2. R. P. Lowe, "Interferometric spectra of the Earth's airglow (1.2 to 1.6- μm)," *Philos. Trans. R. Soc. London Ser. A* **264**, 163–169 (1969).
3. R. J. Thomas, C. A. Barth, D. W. Rusch, and R. W. Sanders, "Solar mesosphere explorer near-infrared spectrometer: measurements of the 1.27- μm radiances and the inference of mesospheric ozone," *J. Geophys. Res.* **89**, 9569–9580 (1984).
4. J. M. Russell, III, M. G. Mlynczak, and L. L. Gordley, "Overview of the Sounding of the Atmosphere Using Broadband Emission Radiometry (SABER) experiment for the Thermosphere-Ionosphere-Mesosphere Energetics and Dynamics (TIMED) mission," in *Optical Spectroscopic Techniques and Instrumentation for Atmospheric and Space Research*, J. Wang and P. B. Hays, eds., Proc. SPIE **2266**, pp. 406–414 (1994).
5. W. A. Traub, N. P. Carleton, P. Connes, and J. F. Noxon, "The latitude variation of O_2 dayglow and O_2 abundance on Mars," *Astrophys. J.* **229**, 846–850 (1979).
6. M. G. Mlynczak and B. T. Marshall, "A reexamination of the role of the solar heating in the O_2 atmospheric and infrared atmospheric bands," *Geophys. Res. Lett.* **23**, 657–660 (1996).
7. M. G. Mlynczak and D. S. Olander, "On the utility of the molecular oxygen dayglow emissions as proxies for middle atmospheric ozone," *Geophys. Res. Lett.* **22**, 1377–1380 (1995).
8. M. G. Mlynczak and D. J. Nesbitt, "The Einstein coefficient for spontaneous emission of the O_2 ($a^1\Delta_g$) state," *Geophys. Res. Lett.* **22**, 1381–1384 (1995).
9. R. M. Badger, A. C. Wright, and R. F. Whitlock, "Absolute intensities of the discrete and continuous absorption bands of oxygen gas at 1.26 and 1.065 μ and the radiative lifetime of the $^1\Delta_g$ state of oxygen," *J. Chem. Phys.* **43**, 4345–4350 (1965).
10. Y. T. Hsu, Y. P. Lee, and J. F. Ogilvie, "Intensities of lines in the band $a^1\Delta_g(v' = 0) - X^3\Sigma_g^-(v'' = 0)$ of $^{16}\text{O}_2$ in absorption," *Spectrochim. Acta* **9**, 1227–1230 (1992).
11. L.-B. Lin, Y.-P. Lee, and J. F. Ogilvie, "Line strengths of the band $a^1\Delta_g(v' = 0) - X^3\Sigma_g^-(v'' = 0)$ of $^{16}\text{O}_2$," *J. Quant. Spectrosc. Radiat. Transfer* **5**, 375–380 (1988).
12. W. R. Pendleton, Jr., D. J. Baker, R. J. Reese, and R. R. O'Neil, "Decay of $\text{O}_2(a^1\Delta_g)$ in the evening twilight airglow: implications for the radiative lifetime," *Geophys. Res. Lett.* **23**, 1013–1016 (1996).
13. R. R. Gamache, A. Goldman, and L. S. Rothman, "Improved spectral parameters for the three most abundant isotopomers of the oxygen molecule," *J. Quant. Spectrosc. Radiat. Transfer* (to be published).
14. C. Amiot and J. Verges, "The magnetic dipole $a^1\Delta_g(v' = 0) - X^3\Sigma_g^-$ transition in the oxygen afterglow," *Can. J. Phys.* **59**, 1391–1398 (1981).
15. Y. Endo and M. Mizushima, "Microwave resonance lines of $^{16}\text{O}_2$ in its electronic ground state ($X^3\Sigma_g^-$)," *Jpn. J. Appl. Phys.* **21**, L379–L380 (1982).
16. K. W. Hillig, II, C. C. W. Chiu, W. G. Read, and E. A. Cohen, "The pure rotation spectrum of $a^1\Delta_g \text{O}_2$," *J. Mol. Spectrosc.* **109**, 205–206 (1985).
17. G. Rouillé, G. Millot, R. Saint-Loup, and H. Berger, "High-resolution stimulated Raman spectroscopy of O_2 ," *J. Mol. Spectrosc.* **154**, 372–382 (1992).
18. 1996 version of the HITRAN database described in L. S. Rothman, R. R. Gamache, R. H. Tipping, C. P. Rinsland, M. A. H. Smith, D. C. Benner, V. Malathy Devi, J.-M. Flaud, C. Camy-Peyret, A. Perrin, A. Goldman, S. T. Massie, L. R. Brown, and R. A. Toth, "The HITRAN molecular database: editions of 1991 and 1992," *J. Quant. Spectrosc. Radiat. Transfer* **48**, 469–507 (1992). A CDROM version of the 1996 database is available from L. S. Rothman, Harvard Observatory, P-248, Harvard University, Cambridge, Mass. 02138.
19. L. Wallace and W. Livingston, "Spectroscopic observations of atmospheric trace gases over Kitt Peak: 1. Carbon dioxide and methane from 1979 to 1985," *J. Geophys. Res.* **95**, 9823–9827 (1990).
20. D. C. Tobin, L. L. Strow, W. J. Lafferty, and W. B. Olson, "Experimental investigation of the self- and N_2 -broadened continuum within the ν_2 band of water vapor," *Appl. Opt.* **35**, 4724–4734 (1996).
21. E. E. Whiting, A. Schadee, J. B. Tatum, J. T. Hougen, and R. W. Nicholls, "Recommended conventions for defining transition moments and intensity factors in diatomic molecular spectra," *J. Mol. Spectrosc.* **80**, 249–256 (1980).
22. E. E. Whiting and R. W. Nicholls, "Reinvestigation of

- rotational-line intensity factors in diatomic spectra," *Astrophys. J. Suppl. No. 235*, **27**, 1–19 (1974).
23. T. K. Balasubramanian and V. P. Bellary, "Intensity distribution in the rotational structure of ${}^1\Delta_{-3}\Sigma$ and ${}^1\Pi_{-3}\Sigma$ transitions in diatomic molecules," *J. Mol. Spectrosc.* **63**, 249–255 (1988).
24. V. P. Bellary and T. K. Balasubramanian, "On the rotational intensity distribution in the $a\ {}^1\Delta_g \rightarrow X\ {}^3\Sigma_g^-$ magnetic dipole transition of oxygen molecule," *J. Mol. Spectrosc.* **126**, 436–442 (1987).
25. G. Herzberg, *Spectra of Diatomic Molecules* (Van Nostrand, New York, 1950), p. 21.
26. R. L. Gattinger and A. Vallance Jones, "Observation and interpretation of O_2 1.27- μ emission enhancements in aurora," *J. Geophys. Res.* **78**, 8305–8313 (1973).
27. W. F. J. Evans, H. C. Wood, and E. J. Llewellyn, "Ground-based photometric observations of the 1.27 μ band of O_2 in the twilight airglow," *Planet. Space Sci.* **18**, 1065–1073 (1970).